X-ray elastic constant determination and residual stress estimation of spherical carbide in JIS SK3

Proceedings of the Sixteenth (2006) International Offshore and Polar Engineering Conference
San Francisco, California, USA, May 28-June 2, 2006

ISBN 1-880653-66-4 (Set); ISSN 1098-6189 (Set)

X-Ray Elastic Constant Determination and Residual Stress Estimation of Spherical Carbide in JIS SK3

Lei Che[1], Masahide Gotoh*[2], Shigeki Takago*[3] and Yukio Hirose*[4]*
*1 Kanazawa University, Kanazawa, JAPAN
*2 VBL, Kanazawa University, Kanazawa, JAPAN
*3 Mechanical Engineering, Industrial Research Institute of Ishikawa, Kanazawa, JAPAN
*4 Kanazawa University, Kanazawa, JAPAN

ABSTRACT

After special surface treatments on specimens, residual stress behaviors of ferrite and cementite phases in two kind sizes of spheroidized JIS SK3 steels after tensile deformation were estimated by X-ray diffraction method. In the study, phase cementite X-ray elastic constant was obtained from composite X-ray elastic constants; compressive residual stresses were observed in ferrite and tensile residual stresses in cementite; the particle size of cementite has obvious affections on the residual stress behaviors of both cementite and ferrite; in order to well understand the interaction between cementite and matrix, the plastic strains of two phases and the misfit of plastic strain between them were analyzed based on Eshelby/Mori-Tanaka model.

KEY WORDS: Cementite; Residual stress; Plastic strain; Surface treatment; X-ray; Eshelby/Mori-Tanaka;

INTRODUCTION

It is well known, carbon in tool steels contributes to several mechanical properties of the tool steel materials. The property of cementite (Fe_3C) that exist in carbon steels as the second phase affects the mechanical properties of carbon steels. In the past, some studies proved that the volume fraction and structure of the cementite will influence the strength and fracture toughness of steels during plastic deformation and cycle fatigue. (Sakamaki,1980,1981;Nishida,1992;Winholtz,1992;Tohgo, 1993) A complete understanding the interactions between ferrite and cementite is helpful for us to understand the mechanical properties of the carbon steel.

Residual stresses are known to generate within the material during manufacturing processes by inhomogeneous plastic deformations at the macroscopic and microscopic scale. Good understanding of the residual stress states of ferrite and cementite phase in dual phase steels can help us to comprehend the interactions between them in order that we can grasp the mechanical properties of steel materials properly. The well established X-ray diffraction technique can be used for determining the residual stress distributions of matrix and second phase in a two-phase composite materials. But for some two phase tool steel material that commonly used, it is difficult to realize the residual stress measurement of cementite phase using conventional X-ray diffraction method due to its' very weak intensity peaks compare with those of ferrite. Due to this reason, the stresses distribution of ferrite in steel has been generally analyzed but the stresses of cementite have been largely ignored in the studies before. (Behnken,1997;Kornmeier,1997;Zöltzer,2000) For two-phase steel materials include cementite, it is therefore important to know the residual stress state of cementite. In some studies as we know, cementite stress measurement can be realized only in some specific ways. Hanabusa (1969,1987,1989) and Nishida (1989) measured the residual stresses of cementite in JIS SK1 & SK3 with a very low diffraction angle ($2\theta \approx 55°$) using the improved X-ray instrument which can realize low-angle measurement but gives large instrumental errors in the measurement. Winholtz and Cohen (1989,1992) realized the stress measurement of cementite using the (250) cementite peak in $148°2\theta$ using very high X-ray power, long measurement time and some attachments. Some researchers considered that synchrotron radiation (S.R) method was more suitable for cementite stress measurement due to its higher power and deeper penetration than X-ray method. (Belassel,1994;Inal,2004)

In the present study, after the special surface treatments on the specimens, residual stress behaviors of ferrite and cementite phases in two kind sizes of spheroidzed JIS SK3 steels after tensile deformation were estimated by conventional X-ray diffraction method. The phase cementite X-ray elastic constant was determined previously using composite cementite elastic constant of {250} plane which was obtained experimentally. At last, the misfits of plastic strain in ferrite and cementite phases were analyzed using the theory based on Eshelby/ Mori-Tanaka model.

X-ray Stress Measurement

The X-ray stress measurement is a method of obtaining surface stresses from calculations based on the change in lattice spacing of crystal. For the multiphase materials, X-ray diffraction method also can be applied to the estimation of macro- and micro stresses in each phase.

We set up the coordinate system as shown in Fig.1, σ_x is the stress in φ direction and ψ is the angle between the normal of diffraction plane and the normal of specimen surface. Based on this coordinate system, the relation between strains and stresses can be described as Eq. 1, where σ_{11}, σ_{22} and σ_{33} are principal stresses.

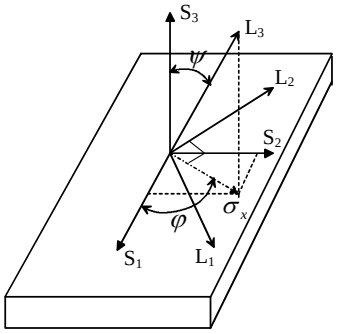

Figure.1 Coordinates of X-ray stress measurement

$$\varepsilon_{33}^{L}=\frac{S_2}{2}(\sigma_{11}\cos^2\varphi+\sigma_{12}\sin 2\varphi+\sigma_{22}\sin^2\varphi)\sin^2\psi+\frac{S_2}{2}\sigma_{33}\cos^2\psi + S_1(\sigma_{11}+\sigma_{22}+\sigma_{33})+\frac{S_2}{2}(\sigma_{13}\cos\varphi+\sigma_{23}\sin\varphi)\sin 2\psi \quad (1)$$

If we only consider the principal stresses and when φ=0,

$$\varepsilon_{33}^{L}=\frac{S_2}{2}(\sigma_{11}-\sigma_{33})\sin^2\psi+\frac{S_2}{2}\sigma_{33}+S_1(\sigma_{11}+\sigma_{22}+\sigma_{33}) \quad (2)$$

where ε_{33}^{L} can be deduced from Bragg's law as follows,

$$\varepsilon_{33}^{L}=-\frac{1}{2}\cot\theta_0(2\theta_\psi-2\theta_0) \quad (3)$$

Equating the Eq.2 and Eq.3, we obtain the following 2θ-sin$^2\psi$ relation,

$$2\theta_\psi=-2\tan\theta_0\left\{\frac{S_2}{2}(\sigma_{11}-\sigma_{33})\sin^2\psi+\frac{S_2}{2}\sigma_{33}+S_1(\sigma_{11}+\sigma_{22}+\sigma_{33})\right\}+2\theta_0 \quad (4)$$

from Eq. 4, the stress $\sigma_{11}-\sigma_{33}$ is determined by the following equation;

$$\sigma_{11}-\sigma_{33}=-\frac{1}{S_2}\cdot\cot\theta_0\cdot\frac{\partial(2\theta_0)}{\partial(\sin^2\psi)}\cdot\frac{\pi}{180} \quad \text{(MPa)} \quad (5)$$

We name S_1 and S_2 as X-ray elastic constants (XEC) and they can be described as follows, E_x and ν_x are X-ray Young's modulus and Poisson's ratio.

$$S_1=-\frac{\nu_x}{E_x},\qquad S_2=\frac{2(1+\nu_x)}{E_x} \quad (6)$$

Defining K and M as

$$K=-\frac{1}{S_2}\cdot\cot\theta_0\cdot\frac{\pi}{180} \quad \text{(MPa/deg)} \quad (7)$$

$$M=\frac{\partial(2\theta_\psi)}{\partial(\sin^2\psi)} \quad (8)$$

Where K is called stress constant and M is the slope of a linear line in the 2θ-sin$^2\psi$ diagram.

THEORY

X-ray Measurement of Micro Stresses and Misfit of Plastic Strain in Two-phase Composite Material

Due to the yield points of the matrix and inclusion are different in composite materials, macro- as well as micro stresses will be generated on a macroscopic and microscopic scale after an applied plastic deformation, as shown in Fig.2. Macro-and micro stresses can be obtained from the phase stress of the matrix σ^M and that of inclusion σ^I

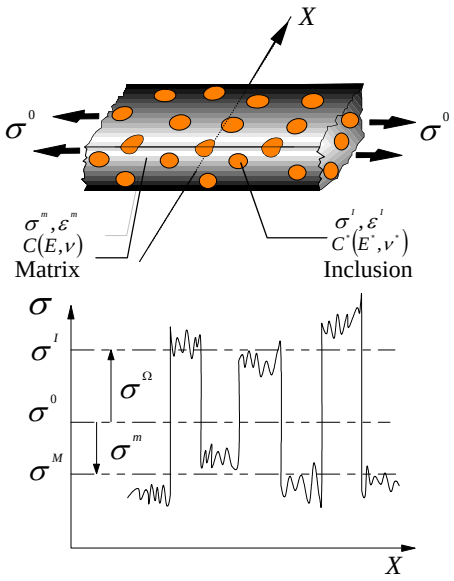

Figure.2 Stress in two-phase composite material

by defining σ^m, σ^Ω as micro stresses in matrix and inclusion.

$$(\sigma_{11}^0-\sigma_{33}^0)=(1-f)(\sigma_{11}^M-\sigma_{33}^M)+f(\sigma_{11}^I-\sigma_{33}^I) \quad (9)$$

where f is defined as the volume fraction of the inclusion, then microstresses of the two phases can be obtained as follows,

$$(\sigma_{11}^m-\sigma_{33}^m)=f\left[(\sigma_{11}^M-\sigma_{33}^M)+(\sigma_{11}^I-\sigma_{33}^I)\right] \quad (10)$$

$$(\sigma_{11}^\Omega-\sigma_{33}^\Omega)=(f-1)\left[(\sigma_{11}^M-\sigma_{33}^M)+(\sigma_{11}^I-\sigma_{33}^I)\right] \quad (11)$$

For two-phase composite materials with homogenous, isotropic matrix and isotropic spherical inclusions, the misfit of plastic strain can be obtained from the Eshelby and Mori-Tanaka method. (Sasaki, 1997)

$$(\sigma_{11}^M-\sigma_{33}^M)=3P\cdot(\sigma_{11}^0-\sigma_{33}^0)-3B_1f\cdot(\Delta\varepsilon_{11}^P-\Delta\varepsilon_{33}^P) \quad (12)$$

$$(\sigma_{11}^I-\sigma_{33}^I)=3P^*\cdot(\sigma_{11}^0-\sigma_{33}^0)+3B_1(1-f)\cdot(\Delta\varepsilon_{11}^P-\Delta\varepsilon_{33}^P) \quad (13)$$

where $\Delta\varepsilon_{ij}^P$ is the misfit of the plastic strain between the matrix and the inclusion .From Eq.12 and Eq.13, $\Delta\varepsilon_{ij}^P$ can be written as the following form:

$$\Delta\varepsilon_{11}^P-\Delta\varepsilon_{33}^P=\frac{P}{Q}(\sigma_{11}^I-\sigma_{33}^I)-\frac{P^*}{Q}(\sigma_{11}^M-\sigma_{33}^M) \quad (14)$$

Phase plastic strains can be obtained as:

$$\varepsilon_{M1}^P-\varepsilon_{M3}^P=-f(\Delta\varepsilon_1^P-\Delta\varepsilon_3^P)+(\varepsilon_1^P-\varepsilon_3^P) \quad (15)$$

$$\varepsilon_{I1}^P-\varepsilon_{I3}^P=(1-f)(\Delta\varepsilon_1^P-\Delta\varepsilon_3^P)+(\varepsilon_1^P-\varepsilon_3^P) \quad (16)$$

The parameters above can be determined as follows,

$$P=\frac{\mu-\beta(\mu-\mu^*)}{3B},P^*=\frac{\mu^*}{3B},Q=B_1\{3P(1-f)+3P^*f\},$$
$$B_1=\frac{2(\beta-1)\mu\mu^*}{3B},\mu=\frac{E}{2(1+\nu)},\mu^*=\frac{E^*}{2(1+\nu^*)},$$
$$B=\mu-\{\beta-f(\beta-1)\}(\mu-\mu^*),\beta=\frac{2(4-5\nu)}{15(1-\nu)} \quad (17)$$

where E and E^* are Young's moduli, ν and ν^* are Poisson's ratios of the matrix and inclusions, respectively.

Here, E =206GPa, ν =0.28 (S.M.S, 2002); E^* =177GPa, ν^* =0.26 (Mizubayashi,1999), they are obtained from literatures.

EXPERIMENTAL PROCEDURES

Material Investigated

The steel used in experiment is JIS SK3. The chemical compositions of this material are listed in Table 1 and the geometry of specimen for tensile experiment is as shown in Fig.3.

Table.1 Chemical composition of JIS SK3 (wt.%)

C	Si	Mn	P	S	Cu	Ni	Cr
1.10	0.29	0.42	0.017	0.008	0.05	0.03	0.12

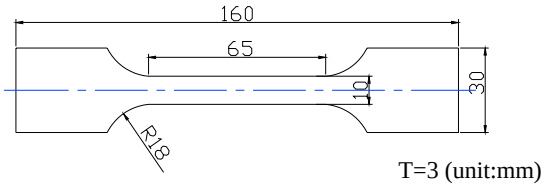

T=3 (unit:mm)

Figure.3 Geometry of tensile specimen

The specimens for tensile experiment have undergone different heat treatments in order to obtain two kinds of micro structure: large size globular cementite structure (GL) and small size globular cementite structure (GS). GL was obtained by spheroidize annealing between 700°C and 770°C ,as shown in Fig.4(a); the material was austenitized at 900°C for 2 hours and oil quenched, thereafter GS was obtained by spheroidize annealing between 700°C and 750°C, as shown in Fig.4(b). The micro structures that we obtained were shown in Fig.5.

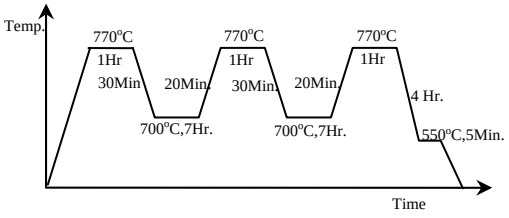

(a) Heat treatment of GL

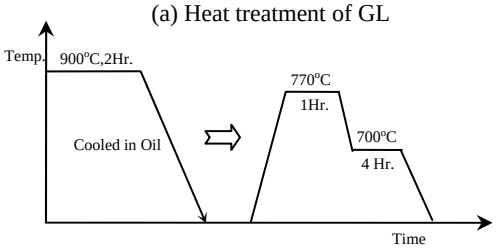

(b) Heat treatment of GS

Figure.4 Heat treatment process

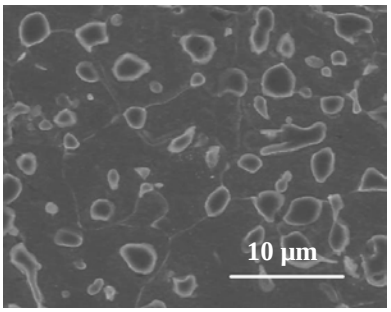

(a) Large globular structure (GL)

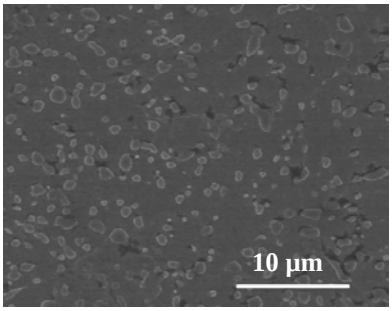

(b) Small globular structure (GS)

Figure.5 Micro structure of specimen

Surface Treatment and X-ray Diffraction Condition

In order to obtain sufficient diffracted intensity of cementite, surface treatments of specimens are indispensable to the X-ray measurement in this study. At first, superficial oxidizing and decarburized layer that generated in the heat treatments (as shown in Fig.6 (a)) was polished by sandpaper and the surface effects induced in this step (Fig.6 (b)) were eliminated by electrochemical polishing (Fig.6 (c)); thereafter the specimen was wet polished using 0.5 µm diameter of alumina polishing powder and the surface residual stresses were limited to not more than 50MPa (Fig.6 (d)); at last, the surface of the specimen was corroded slightly by HNO_3 + CH_3OH liquid(Fig.6 (e)). The final state of specimen for X-ray measurement was shown in Fig.7.

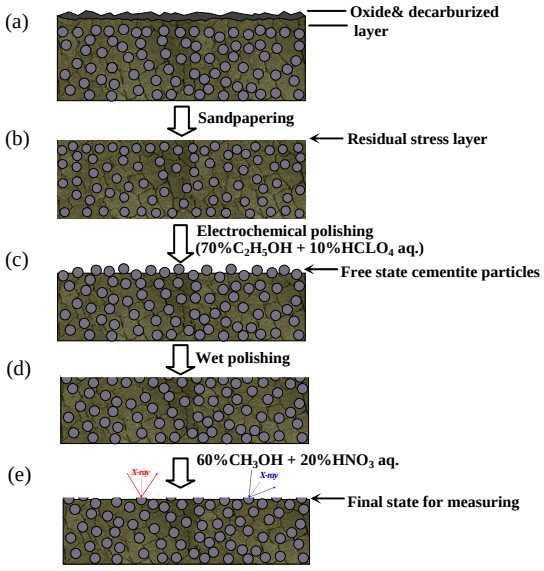

Figure.6 Surface treatment procedure

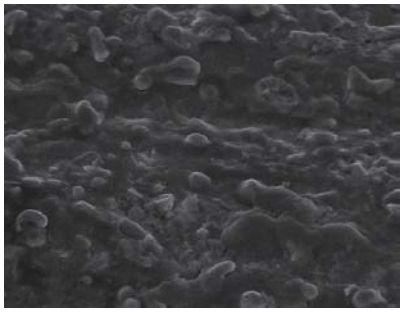

Figure.7 Final state of specimen after surface treatment

Using the above procedure and under the conditions that summarized in Table 2, we obtained the cementite peak as shown in Fig.8 and succeeded in X-ray stress measurement of cementite. The whole stress measurement time of cementite is about 3 hours.

Table.2 Conditions of X-ray diffraction experiment

	α-Fe	Cementite
Characteristic X-ray	Cr-K_α	
Measure method	Ω-diffractometer method	
Diffraction plane, hkl	211	250
K_β-Filter	V	None
Tube voltage, KV	30	
Tube current, mA	10	
Diffraction angle, deg	156.4	148.1
Peak position	H.V.B	Gaussian

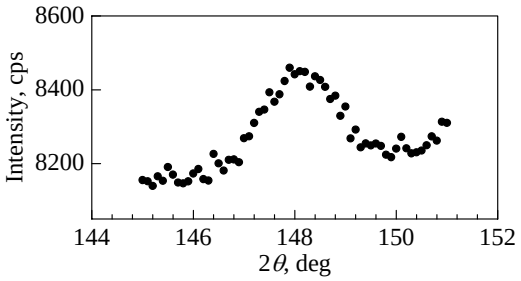

Figure.8 Intensity of the 250 cementite peak (ψ=0)

RESULTS AND DISCUSSION

X-Ray Elastic Constant Determination

The composite X-ray elastic constants (CXEC) of cementie and ferrite phases were determined by 4-point bending experiment. The CXEC determination is based on the lattice strain ε measurement by $\sin^2\psi$ method under different applied loading stresses 0,60,120 and 180 MPa. The slopes of M and $2\theta_{\psi=0}$ and intercept with applied stress for 250 cementite diffraction are shown in Fig.9.

In the stress calculation of each phase in composite materials, the phase X-ray elastic constants (PXEC) are required. In this study, the PXEC of cementite phase is obtained by the method (Tanaka,1990) as follows,

$$\frac{\left(S_2^I\right)_{composite}}{\left(S_2^I\right)_{phase}}\cdot f+\frac{\left(S_2^M\right)_{composite}}{\left(S_2^M\right)_{phase}}\cdot\left(1-f\right)=1$$

where $\left(S_2^M\right)_{composite}$ and $\left(S_2^I\right)_{composite}$ are the CXEC of ferrite and cementite respectively and they can be obtained from Fig.9; $\left(S_2^M\right)_{phase}$ was calculated using the Kröner model with the elastic compliance of ferrite single crystal and equal to 11.41×10^{-6} MPa^{-1}; the volume fraction of cementite f was determined by point count method, and f = 0.16 ± 0.0010 for GL, f =0.15±0.0028 for GS.

The XEC and K of ferrite phase for the {211} plane and cementite phase for the {250} we obtained are listed in Table 3. We obtained approximate $(S_2)_{phase}$ values of cementite which were calculated from $(S_2)_{composite}$ of GL and GS individually.

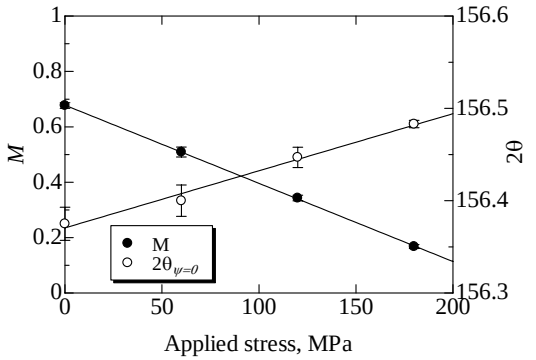

(a) Ferrite of GL

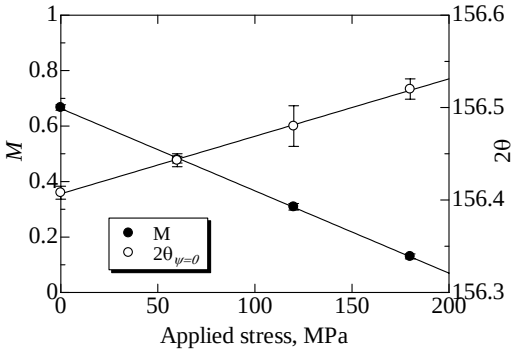

(b) Ferrite of GS

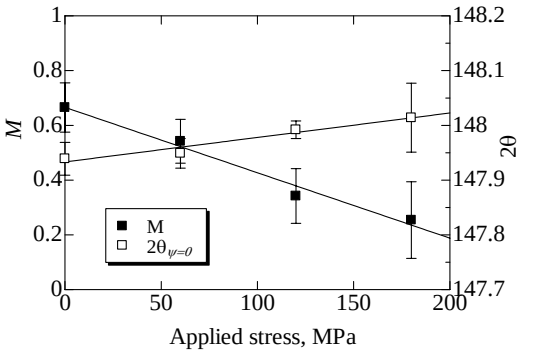

(c) Cementite of GL

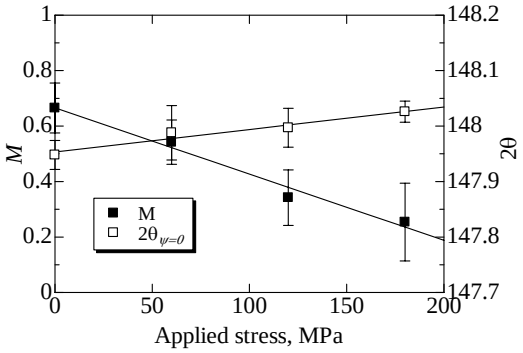

(d) Cementite of GS

Figure.9 Slope of M and $2\theta_{\psi=0}$ and intercept with applied stress for 250 cementite

Table.3 XEC and K of SK3. (S_1, S_2: 10^{-6} MPa^{-1}, K: MPa/deg)

Phase		$(S_1)_{composite}$	$(S_2)_{composite}$	$(S_2)_{phase}$	K
Ferrite	GL	-1.17±0.05	10.5±0.1	11.41	-319.3
	GS	-1.21±0.07	10.8±0.1	11.41	-319.3
Cementite	GL	-0.80±0.07	10.7±0.3	7.56	-661
	GS	-0.79±0.04	10.4±0.2	8.01	-624

Micro Stresses and Misfit of Plastic Strain after Tensile Plastic Deformation

In this study, the relations between stress evolutions and applied plastic strains were obtained after tensile plastic deforming and unloading in ferrite and cementite phases. Macro stresses and phase stresses in globular cementite structure were shown in Figure 10 and Figure 11, respectively. GL and GS have the parallel behaviors of residual stress evolution. In the material, compressive residual stress was observed in ferrite phase and tensile one in cementite. The residual stresses in cementite phase are much higher than those in ferrite phase. In the globular structure cementite, the residual stresses in GS are higher than those of GL, the residual stress values of GL and GS are approximately in the ferrite phase. The phase residual stress of cementite in GL increases with applied plastic strains till about 3.5%, and decreases with subsequent strains thereafter. We named the strain value from where the stress in cementite begins to decrease as the border strain point (BSP). For GS, the emergence of BSP is earlier than GL, and it is about 2.7%.

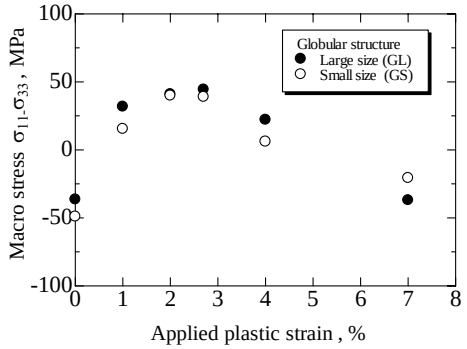

Figure.10 Macro stress

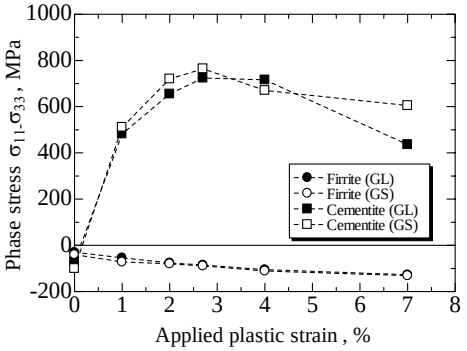

Figure.11 Phase stress

In Figure 12, it can be observed, for GL and GS, the micro stresses in not only cementite but also ferrite decrease simultaneously when the applied plastic strain value exceed the BSP. The evolution behaviors of micro plastic strains in two phases, as shown in Figure 13, are as same as that of the micro stresses. Figure 14 is the misfit of plastic strain between ferrite and cementite phases. The misfit of plastic strain between two phases also decreases when the applied plastic strains exceed the BSP. In Figure 15, it can be observed that the increase tendencies of the phase plastic strains in cementite and ferrite are curvilinear before the applied strain arrives at the BSP, and are linear thereafter.

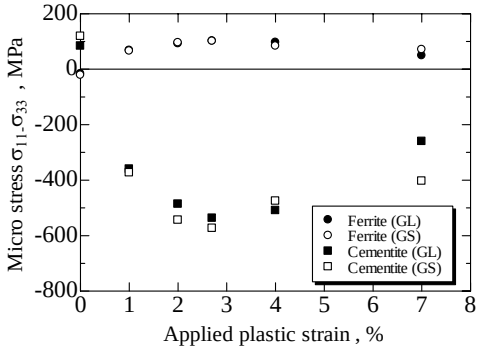

Figure.12 Micro stress

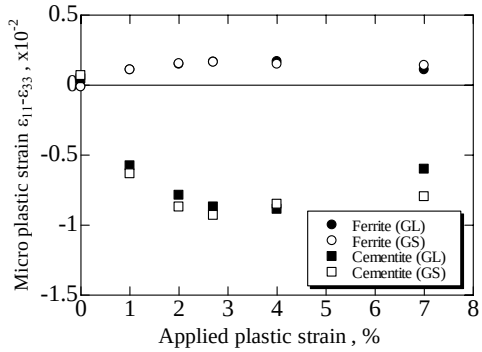

Figure.13 Micro plastic strain

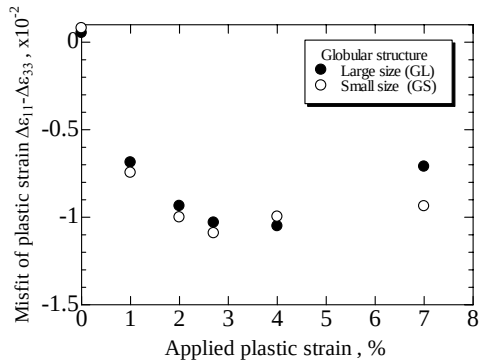

Figure.14 Misfit of plastic strain

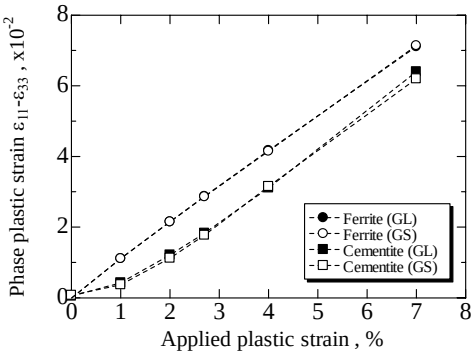

Figure.15 Plastic strain

From the above experimental results we can observe that not only the stress in cementite phase but also the misfit of plastic strain between cementite and ferrite phase decrease after the applied plastic strains exceeds the BSP. D.A.Porter (1978) explained this phenomenon as: dislocations pile up at the interface that causes a high shear stress level leading to a fracture of the cementite. In our study, scanning electron microscopy was used to observe the reasons which induce to the decrease of residual stress in cementite phase. We find two reasons which may induce the decrease of residual stress in cementite, one is the particle cracking at the cementite (Fig.16 (a)), and the other is the crack separation at the boundary between cementite particle and matrix. (Fig.16 (b)). The mechanism of crack generation inside cementite particle and on the boundary will be discussed in detail in our subsequent paper.

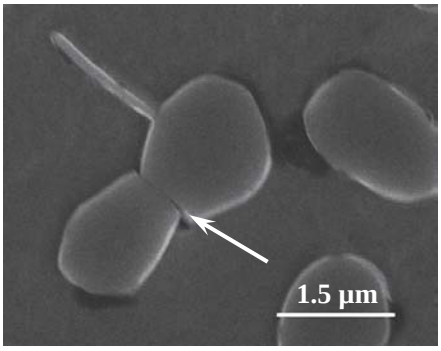

(a) Crack in cementite particle

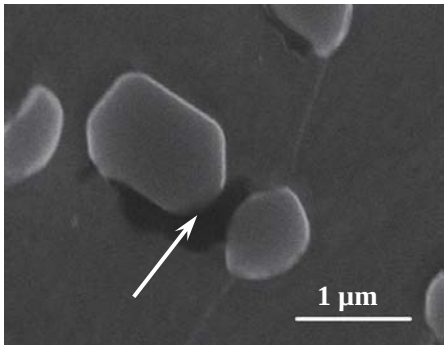

(b) Crack separation between cementite particle and matrix
Figure.16 Crack in particle and at the boundary

CONCLUSIONS

(1)After the surface treatments of specimen, sufficient intensity of (250) diffracted peak of globular structure cementite was obtained and makes it possible to realize the X-ray residual stress measurement of cementite.
(2)PXEC of cementite was determined by the CXEC which can be obtained experimentally.
(3)The residual stress distribution in ferrite and cementite depends on the microstructures of carbon steels; the stress in cementite phase is much higher than that in ferrite phase and stress of cementite in GL is higher than that in GS; the stress of cementite phase decreases after applied plastic strain exceeds the BSP.
(4)The crack in cementite particle and the crack separation at the boundary between cementite particle and matrix may induce the decrease of residual stress in cementite.

ACKNOWLEDGEMENT

The authors would like to thank Mr. H.Shimazaki (Undergraduate school, Kanazawa University) sincerely for his contributive assistance in preparing specimens.

REFERENCES

Belassel, Ji and Lerun (1994).“Analysis of the Mechanical Behavior of Materials Through the 2nd and 3rd Order Stress Determination”, *Jounal De Physique IV*, C9, pp261-264.

Belassel, Lebrun and Denis (1994). “Effect of Thermal and Mechanical Loading on the Generation of Macro and Micro Stresses in Eutectoid Steel”, *International Conf. on Residual Stresses 4*, Bethel, pp392-401.

Behnken, Hauk (1997). “Residual Stress State after Uniaxial Deformation”, *International Conf. on Residual Stresses 5*, Linköping, Sweden, pp539-544.

Hanabusa, Fukura and Fujiwara (1969). “X-Ray Residual Stress Measurement of Cementite in Steel Material”, *J.S.M.E.*, Vol.35, pp237-244.

Hanabusa, Fujiwara and Uga (1987). “Development of Residual Stress in Deformed Steel Containing Carbide Particles”, *Residual Stress in Science and Technology*,Vol.1, pp547-554.

Hanabusa, Fujiwara and Nishida (1989). “Residual Microstress Development in Steels after Tensile Deformation”, *International Conf. on Residual Stresses 2*, Elservier Apllied Science, London and New York, pp555-560.

Inal, Lebrun and Belassel (2004). “Second-Oder Stresses and Strains in Heterogeneous Steels: Self-Consistent Modeling and X-Ray Diffraction Analysis”, *Metallurgical and Materials Transactions A*, Vol.35A, pp2361-2369.

Kornmeier, Scholtes and Dias (1997). “Residual Stress in Perlitic Steel with Different Cementite Shape after Plastic Deformation Analysed by Mechanical and X-ray Methods”, *International Conf. on Residual Stresses 5*, LinkÖping, Sweden, pp545-550.

Mizubayashi, Li, and Yumoto, et al. (1999). “Influence of Alloy Additions on Production and Properties of Bulk Cementite”, *Scripta Materialia*, Vol.40, pp773-777.

Nishida, Hanabusa and Fujiwara (1989). “Residual Microstress Development in Two-Phase Materials Due to Tensile Deformation”, *J. Soc. Mat. Sci., Japan*, Vol.38, pp576-581.

Nishida, Mutoh and Tsujii (1992). “Effect of Size and Volume Fraction of Cardide Particles on Strength and Fracture Toughness of P/M High Speed Steel”, *J. Soc. Mat. Sci., Japan*, Vol.41, pp1403-1409.

Porter, Easterling and Smith (1978), “Dynamic Studies of the Tensile Deformation and Fracture of Pearlite”, *Acta Metallurgica*, Vol.26, pp1405-1410.

Sakamaki, Inada (1980). “Brittle Fracture of Lamellar Pearlite Steel Containing Proeutectoid Cementite”, *J.Soc.Mat.Sci., Japan*, Vol.29, pp381 -386.

Sakamaki, Inada and Hori (1981). “Tensile Fracture of Spheroidized 0.7% Carbon Steel at Low Temperatures”, *J.Soc.Mat.Sci., Japan*, Vol.30, pp1109-1115.

Sasaki, Lin, and Hirose (1997). “X-Ray Measurement of Plastic Strain by Means of Eshelby/Mori-Tanaka Model and Its Application”, *J.S.M.E.*, Vol.63 (A), pp158-165.

Society of Material Science, Japan (2002). *X-ray Measurement Standard*, pp61.

Tanaka, Mine, and Suzuki (1990). “X-Ray Study of Elastic Deformation of Zirconia-Alumina Composite”, *J.Soc.Mat.Sci.Japan* ,Vol.39, pp1235-1241.

Tohgo, Ishii and Hiramatsu (1993). “Influence of Cementite Volume Fraction on Mechanical Properties and Fracture Toughness in Spheroidized Cementite Steel”, *J.S.M.E.*, Vol.59 (A), pp1617-1623.

Winholtz, Cohen (1992). “Load Sharing of the Phases in 1080 Steel during Low-Cycle Fatigue”, *Metallurgical Transactions A*, Vol 23A, pp341-354.

Winholtz, Cohen (1989).“Separation of the Macro- and Micro-Stresses in Plastically Deformed 1080 Steel”, *Adv. X-ray Anal.*, Vol.32, pp341- 353.

Winholtz, J.B.Cohen (1992). “Changes in the Macrostresses and Microstresses in Steel with Fatifue”, *Mater. Sci. Eng.* A154, pp155 -163.

Zöltzer, Scholtes (2000). “Analysis of Residual Stresses in Plastically Deformed Plain Carbon steels”, *International Conf. on Residual Stresses 6*, Oxford, U.K, pp171-178.